On the Existence of Spurious Modes in Battle–Lemarie Based MRTD

Costas D. Sarris and Linda P. B. Katehi, *Fellow, IEEE*

***Abstract*—A distinction between the effects of inaccuracy of the Battle–Lemarie wavelet based multiresolution time domain (W-MRTD) scheme for high spatial frequencies and spurious modes is drawn and explained in this letter. Investigating the performance of the scheme under various excitation methods, it is concluded that what was described earlier in the literature as a spurious mode effect actually corresponds to alias frequencies stemming from the excitation of higher order modes by the wavelets, given that the latter are spectrally supported at higher wavenumbers.**

***Index Terms*—MRTD, multiresolution analysis, numerical dispersion.**

I. Introduction

SINCE its original introduction to the field of time domain microwave circuit characterization [1], multiresolution analysis has attracted a wide interest among researchers, prompting the formulation of several numerical techniques and the investigation of different wavelet bases. In addition, the dispersion analysis of the Battle–Lemarie wavelet based multiresolution time domain (W-MRTD) scheme (in [1], [2]) has demonstrated its high linearity, that practically allows for a relatively coarse discretization rate. However, little attention has been devoted to the explanation of the dispersion properties of MRTD, by connecting its numerical performance to wavelet theory elements and thus gaining better understanding of its advantages but also its limitations. In this letter, a comprehensive interpretation of the dispersion behavior of W-MRTD, including the "spurious mode" effect which was cited in [1], is provided. Using the result of a one-dimensional dispersion analysis, validated by a simple numerical example, it is concluded that there are strictly no spurious modes in W-MRTD.

II. Dispersion Analysis

A one dimensional case is chosen as an appropriate vehicle for the intelligible presentation of the subtle aspects of this work. In particular, the equations

$$\frac{\partial}{\partial t} E_z(x, t) = \frac{1}{\epsilon} \frac{\partial}{\partial x} H_y(x, t) \tag{1}$$

$$\frac{\partial}{\partial t} H_y(x, t) = \frac{1}{\mu} \frac{\partial}{\partial x} E_z(x, t) \tag{2}$$

are considered and discretized following the moment method based technique of [1]. As an example, keeping the notation in consistence with [1], the electric field component E_z is first expanded in terms of Battle–Lemarie scaling $\{\phi_m\}$ and wavelet $\{\psi_m\}$ functions in space and pulse functions h_n in time:

$$E_z(x, t) = \sum_{n,m} \{{}_nE_m^{z,\phi}\phi_m(x) + {}_n E_m^{z,\psi}\psi_m(x)\}h_n(t) \tag{3}$$

m, n being space cell and time step indices respectively. Subsequently, the discretization of (1) and (2) via Galerkin's method leads to update equations with respect to electric and magnetic field scaling and wavelet expansion coefficients, of the generic form

$$\begin{aligned} {}_{n+1}E_m^{z,\chi} = {}&{}_nE_m^{z,\chi} \\ &+ \frac{\Delta t}{\epsilon \Delta x} \sum_{p=-p_0}^{p_0-1} \alpha^{\chi}(p)\, {}_{n+1/2}H_{m+p+1/2}^{y,\phi} \\ &+ \frac{\Delta t}{\epsilon \Delta x} \sum_{p=-p_0}^{p_0-1} \beta^{\chi}(p)\, {}_{n+1/2}H_{m+p+1/2}^{y,\psi} \end{aligned} \tag{4}$$

with $\chi = \phi, \psi$ for the electric field and of a similar (dual) form for the magnetic field. The weighted sums in (4) represent the spatial differentiation operator in the Battle–Lemarie basis and include p_0 grid points to the left and to the right of a scaling/wavelet field node, that are allowed to contribute to its update (for a certain accuracy). The coefficients of these sums are given in [1].

For the dispersion analysis of this scheme, the conventional Fourier method [4] is adapted to the case of a multilevel basis, as described extensively in [3]. In particular, by Fourier transforming electric and magnetic field expansions, the expansion coefficients are expressed as inverse Fourier transforms, in terms of their spatio-temporal harmonics $\tilde{E}^{\phi,\psi}(k, \omega)$, $\tilde{H}^{\phi,\psi}(k, \omega)$. Explicitly determining the latter, yields

$$\left\{\tilde{E}^{\phi}, \tilde{H}^{\psi}\right\} = \mathcal{R}^{\psi}\left\{\tilde{E}^{\phi}, \tilde{H}^{\phi}\right\}, \quad \mathcal{R}^{\psi} = \hat{\psi}(-k)/\hat{\phi}(-k) \tag{5}$$

where $\hat{}$ denotes a Fourier transform. Equivalently, the dispersion relation can be derived by substituting in any two of the four update equations

$${}_k\Lambda_q^{\phi} = \tilde{\Lambda}^{\phi} e^{-i(qX + k\Omega)}, \quad {}_k\Lambda_q^{\psi} = \mathcal{R}^{\psi}{}_k\Lambda_q^{\phi} \tag{6}$$

where $\Lambda = E, H$, $q = m(\pm 1/2)$, $k = n(\pm 1/2)$ and also $X = k\Delta x$, $\Omega = \omega \Delta t$ are normalized wavenumber and frequency variables. Thus formulating a homogeneous system and

Manuscript received November 6, 2000; revised December 23, 2000. This work was supported by the U.S. Army Research Office (DAAD19-00-1-0173).

The authors are with the Radiation Laboratory, Department of Electrical Engineering and Computer Science, University of Michigan, Ann Arbor, MI 48109-2122 USA (e-mail: ksarris@umich.edu).

Publisher Item Identifier S 1531-1309(01)03043-4.

requiring that it admit nontrivial solutions, leads to an expression of the form

$$\det \mathcal{M}(X, \Omega) = 0 \tag{7}$$

where $\mathcal{M}(X, \Omega)$ is the system matrix. This procedure yields the $X = X(\Omega)$—dispersion relationship which is plotted in Fig. 1, along with the S-MRTD case, for $\nu = (1/\sqrt{\epsilon\mu})\Delta t/\Delta x = 0.159\,25$ and stencil $p_0 = 9$. Compared to the W-MRTD dispersion diagrams of [1], the one in Fig. 1 has a single branch instead of two branches. This is a consequence of using a modified Fourier method in our analysis and employing the relationship of the Fourier transform of scaling and wavelet functions to reduce the dimensionality of (7). In fact, the additional branch of the dispersion diagram of [1] corresponds to modes that are not excited in an MRTD mesh, as a derivation of their corresponding eigenvectors can show [3].

In order to theoretically estimate the performance of W-MRTD based on the results of this dispersion analysis, the spectral (wavenumber) domain form of the Battle–Lemarie scaling and wavelet functions [$|\widehat{\phi}(k)|$, $|\widehat{\psi}(k)|$ respectively], depicted in Fig. 2, is inspected. It is noted that the "knee" of the W-MRTD dispersion curve (or its *effective* Nyquist limit) is at $X_{th} \approx 1.6\pi$ (its exact value is stencil-dependent). Furthermore, the intervals $|X| \leq \pi$ and $\pi \leq |X| \leq 2\pi$ define the 3 dB bandwidth for $\hat{\phi}$ and $\hat{\psi}$ respectively. Hence, if the initial data (excitation) is composed of a wavelet function, the range of the simulated wavenumbers extends beyond the effective Nyquist limit of the scheme and therefore, frequencies that correspond to wavenumbers above X_{th} fold back, appearing at low frequency images of theirs (aliasing). However, this is *not* a spurious mode effect and is rather equivalent to what would happen if an FDTD scheme were used to simulate wavenumbers above its Nyquist limit ($X \geq \pi$).

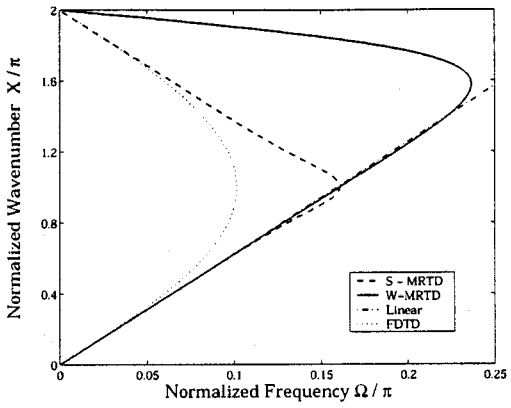

Fig. 1. Dispersion curves for S-MRTD and W-MRTD. FDTD and linear dispersion relationships are shown for comparison.

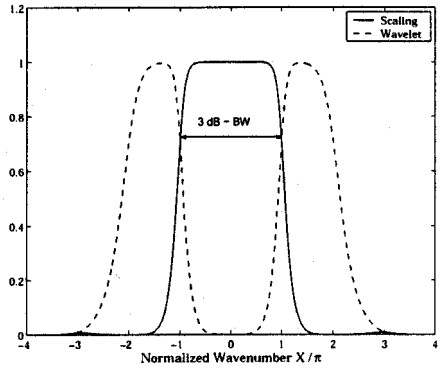

Fig. 2. Spectral domain representation of Battle–Lemarie scaling and mother wavelet function. Evidently, $X = \pm\pi$ is the 3-dB point for both $|\hat{\phi}|$, $|\hat{\psi}|$.

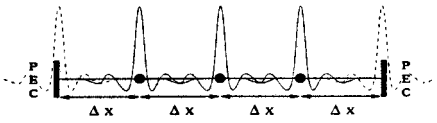

Fig. 3. Computational domain for the 1-D case study.

III. Numerical Results

For the purpose of supporting the conclusion of our dispersion analysis that no spurious modes exist in W-MRTD and to provide a framework of understanding for phenomena that were misconstrued as such, a simple numerical experiment with easily reproducible results and comparable to the one presented in [1] is analyzed. In particular, the one dimensional case study of a domain with four cells defined by three interior scaling functions for the electric field, as shown in Fig. 3, is considered. The hard boundary conditions are imposed by means of image theory and therefore, boundary scaling function terms (shown in Fig. 3 with dashed lines) are set equal to zero (because they are even symmetric with respect to the hard boundary). Electric field wavelet and magnetic field terms are accordingly defined.

Initially, this 1-D cavity is excited by a scaling function placed in the middle of the domain. The field is sampled at integer nodes of the domain and that is why the fourth and the eighth mode (for which $X = \pi, 2\pi$) are not extracted in any case. By Fourier transforming the time domain data, the electric field magnitude in the frequency domain is computed and plotted in Fig. 4 with a continuous line. As expected, modes corresponding to wavenumbers $X < \pi$ are mainly excited, while higher order modes are also excited at significantly lower magnitudes, due to the spectral "tail" of the scaling function beyond $X = \pi$. It is noted that the result of this experiment confirms the absence of the modes corresponding to the second branch of the W-MRTD dispersion diagram of [1] and is consistent with the dispersion analysis of this work.

Next, a scaling and a wavelet function are used as an excitation. Now that the spatial frequencies of the initial data extend from $X = 0$ to 2π, all six modes ($n = 1$ 2, 3 and 5, 6, 7) are almost equally excited. The corresponding electric field spectrum is indicated in Fig. 4 by a dashed line. The mode denoted by $N = 7$ in this figure may be interpreted as spurious. In fact, it comes from the inaccurate determination of the seventh mode by the scheme, the error being equal to -25.692%. It is noted though, that when the excitation is properly confined to spatial frequencies lower than X_{th}, this mode is limited to an insignificant level, as the scaling excitation test case

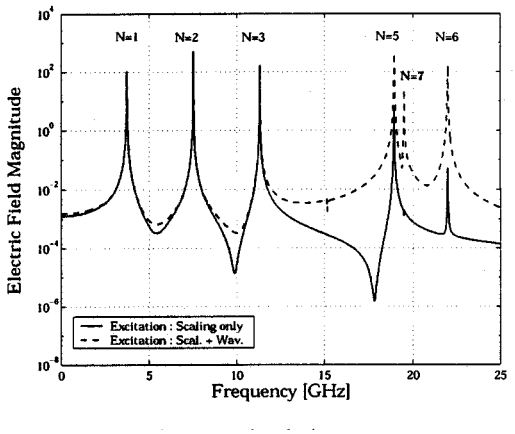

Fig. 4. Semi-logarithmic plot of the electric field magnitude for the case study of Fig. 3, under scaling (—: continuous line) and scaling and wavelet (- -: dashed line) excitation.

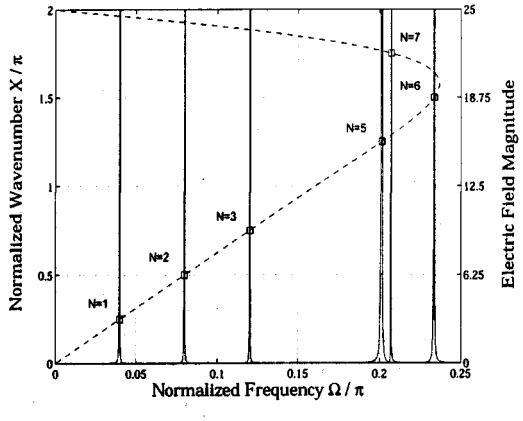

Fig. 5. Field magnitude for the 1-D case study and normalized wavenumber (according to the W-MRTD dispersion relation) as a function of frequency.

suggests. A graphical presentation of these arguments is provided by Fig. 5, where the spectrum of the electric field, when a scaling and wavelet excitation is used, is plotted along with the W-MRTD dispersion curve. Evidently, each resonant frequency can be assigned to the wavenumber of one of the six excited modes, given by $X = n\pi/4$, $n = 1, 2, 3, 5, 6, 7$. It is also shown that the numerical results of the simulation are in absolute agreement with the theoretical prediction of the dispersion behavior of the scheme. Thus, it is concluded that the single branch of Fig. 1 fully describes the W-MRTD dispersion

TABLE I
RESONANT FREQUENCIES (IN GHz) AND RELATIVE ERROR (1-D CAVITY/SCALING + WAVELET EXCITATION)

n	f_n	W-MRTD	ERROR (%)
1	3.747	3.750	+0.081
2	7.518	7.495	+0.305
3	11.312	11.242	+0.628
4	14.990	15.130	+0.935
5	18.737	18.938	+1.074
6	22.484	21.981	-2.237
7	26.232	19.492	-25.692

properties. As for the seventh mode resonant frequency, it is observed that since its corresponding wavenumber is above the effective Nyquist limit of W-MRTD, it is reflected on its alias, just in front of the fifth mode resonant frequency. Finally, numerical values for all points that are indicated in Fig. 5, comparing analytical resonant frequencies to W-MRTD resonant frequencies are given in Table I.

IV. CONCLUSIONS

A W-MRTD dispersion analysis, consistently confirmed by numerical results, showed that there are strictly no spurious modes in this scheme, despite earlier claims of the opposite. Then, the source of misconstruction was identified as being the fact that an effective Nyquist limit for W-MRTD is located within the support of the Battle–Lemarie wavelet function. Therefore, a delta type excitation of wavelet terms excites modes with wavenumbers above X_{th} that eventually produce alias frequencies and corrupt the performance of the scheme. Properly restricting the excitation within the range of W-MRTD dispersion linearity allows for the accurate simulation of microwave structures at relatively coarse discretization rates.

REFERENCES

[1] M. Krumpholz and L. P. B. Katehi, "MRTD: New time domain schemes based on multiresolution analysis," *IEEE Trans. Microwave Theory Tech.*, vol. 44, pp. 555–561, Apr. 1996.

[2] E. Tentzeris, R. Robertson, J. Harvey, and L. P. B. Katehi, "Stability and dispersion analysis of Battle–Lemarie based MRTD schemes," *IEEE Trans. Microwave Theory Tech.*, vol. 47, pp. 1004–1013, July 1999.

[3] C. D. Sarris and L. P. B. Katehi, "Some aspects of dispersion analysis in MRTD schemes," in *Proc. 2001 Review of Progress in Applied COmputational Electrmagnetics Conf.*, Monterey, CA.

[4] A. Taflove, *Computational Electrodynamics: The Finite Difference Time Domain Method*. Norwood, MA: Artech House, 1995, ch. 5.